Thermo-mechanical modelling for prediction of residual stresses in laser powder bed fusion fabricated Ti6Al4V components

G. C. Akshay Kiran[*], N. Ramesh Babu

Indian Institute of Technology Madras, Chennai, India

ABSTRACT

Additive Manufacturing, mainly the LPBF process, can be used to fabricate valuable components for aerospace applications, including parts for Launch Vehicles. This would significantly reduce the number of parts in the assembly, time, and cost. However, the rapid heating and cooling cycles in an LPBF process result in residual stresses in the fabricated components, limiting their usage. To achieve dimensional accuracy and to prevent premature fatigue failure of components, it is essential to get a reasonable estimation of the residual stresses induced in the component. The development of Thermo-Mechanical models for their estimation is of utmost importance since numerous process variables influence the amount of residual stress created during the LPBF process, and experimental measurement of residual stresses is time-consuming and expensive. In the present study, an attempt has been made to study the effect of preheating on the residual stresses using the developed Thermo-Mechanical model.

1. Introduction

The Laser Powder Bed Fusion (LPBF) process can be used to fabricate critical and complex-shaped aerospace components, including Launch Vehicles components, in the shortest possible time at a reduced cost. This has the capability to accelerate the pace of the Space sector further. LPBF process uses a high-powered laser to completely melt powder particles layer by layer and transform them into 3D components. This layer-by-layer melting in an LPBF process induces residual stresses in the fabricated parts. These residual stresses are induced due to the large thermal gradients generated within the component due to the rapid heating and cooling cycles taking place in the process. This tensile residual stress build-up in the parts can lead to catastrophic failure of the component due to distortion, delamination, or cracking.

In the present investigation, an effort has been made to predict the residual stresses induced in a Ti6Al4V component using a decoupled Thermo-Mechanical model. Further investigation is done using the FE models to predict how the

variation of crucial process parameters like the preheating temperature affects the build-up of residual stresses in the fabricated parts.

2. Modelling Methodology

A thermo-mechanical FE analysis was done in ABAQUS using the decoupled modelling approach. In this approach, we first perform the FE analysis on the thermal model. We then feed the nodal temperature data from the thermal simulation into the mechanical model to perform the stress deformation analysis. Both Thermal and Mechanical FE models were subdivided into multiple layers of dimension 1200×600 μm, each having 50μm thickness. The deposition of the powder layer with time is modelled using the "element birth and death" technique. ABAQUS-DC3D8 heat transfer element was used for the Thermal model, and the C3D8 3D stress element was used for the mechanical model. For the powder layer, both the Thermal and Mechanical FE models use a mesh size of 22.5× 22.5×25 μm. Biased meshing was used for the build platform, with a higher mesh density near the region of the layers and a lower mesh density away from the layers, as shown in Fig. 1. This was done to reduce the number of mesh elements and computational time. Solid bulk Ti6Al4V was selected as the base

material. The scan strategy used in the simulation is illustrated in Fig. 2. The laser beam was programmed to scan six parallel tracks along the x-axis, each measuring 1.2 mm in length. A hatch spacing of 0.1 mm was used in the simulation.
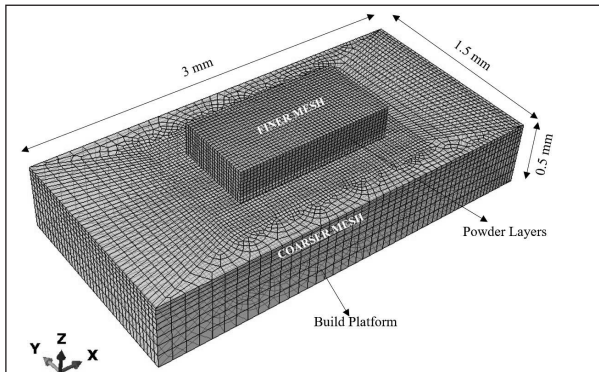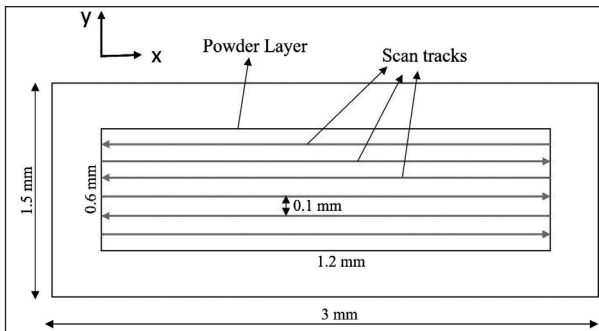

Fig. 1. 3D meshed FEA model.

Fig. 2. Scanning strategy used in the simulations.

2.1 Thermal model

- Thermal Equilibrium

For a thermal model, the governing energy balance equation is given by the heat conduction equation.

$$\rho C_p \frac{dT}{dt} = -\nabla \cdot \mathbf{q}(r, t) + Q(r, t) \qquad \ldots\ldots\ldots\ldots(1)$$

where T is the temperature in Kelvin, $\nabla \cdot$ is the divergence, q is the heat flux, r is the relative reference coordinate, ρ is the density, C_p is the specific heat, and Q is the body heat source. Fourier's conduction equation defines the distribution of heat through the part (Gouge, 2018).

$$\mathbf{q} = -k\nabla T \qquad \ldots\ldots\ldots\ldots(2)$$

where k is the isotropic temperature-dependent thermal conductivity of the material. The initial chamber temperature (initial condition) was set at 40°C. The preheat temperature of the build plate was varied as per the FE model's requirement.

- Heat Input Model

To accurately simulate the LPBF process, we require a reliable and computationally efficient heat input model to reproduce the laser heat source. Beam Scale Exponentially Decaying Model proposed by Liu (2019) was used as the volumetric heat input model. The Beam Scale ED model is a 3D Gaussian Distribution model with its power density decaying exponentially in the depth direction. The input heat flux of the ED model is given by:

$$\mathbf{q} = \frac{2P\eta}{\pi r^2 H} e^{\left(-2\frac{x^2+y^2}{r^2}\right)} e^{-\left(\frac{|z|}{H}\right)} \qquad \ldots\ldots\ldots\ldots(3)$$

where q is the input heat flux in W/m^2, P is the laser power, taken as 200 W, η is the absorption coefficient for Ti6Al4V, taken as 0.65, H is the powder layer thickness, taken as 50μm, and r is the laser spot size, taken as 100μm. DFLUX subroutine written in Visual Studio IDE was used to program the characteristics and movement of the laser heat source in the thermal model.

- Material properties

An accurate representation and description of the temperature-dependent material properties are essential to adequately capture and predict the powder-liquid-solid phase changes in the LPBF process. USDFLD subroutine written in Visual Studio IDE was integrated with the DFLUX subroutine and used to program the phase changes in the process. Thermo-Physical properties of solid Ti6Al4V and powder Ti6Al4V (for a packing factor of 0.6) were taken from the experiments of (Parry et al., 2016; Alderson (2012). Thermo-Physical properties of liquid Ti6Al4V were taken from the experiments of (Boivineau et al., 2006). The powder bed was modelled using the continuum approach. In the thermal model, we have employed the enhanced isotropic thermal conductivity approach suggested by Safdar et al. (2013) to account for the melt-pool convection by multiplying the thermal conductivity of the liquid phase by a factor of 2 to get the required melt-pool dimensions.

- Boundary heat losses

Heat losses may occur during the LPBF process due to conduction, convection, and radiation. Significant heat loss takes place because of heat conduction from the part to the build plate and surrounding powder. For smaller builds,

convection and radiation heat losses are usually neglected for computational efficiency, but we have considered them in our work for more accurate results. To account for the convection losses from the build surface, we have assumed a convective heat transfer coefficient of 20 W/m²°C based on the calibration studies by (Dunbar et al., 2016). In the LPBF process, radiation heat losses are negligible and may be neglected to avoid convergence errors. However, instead of neglecting it completely, we have approximated the temperature-dependent emissivity of Ti6Al4V as a single value of 0.6. To simulate conduction heat losses from the outer surfaces of the layers to the surrounding powder, the modelling reduction approach proposed by (Ali et al., 2018) was used. This approach makes use of the Ti6Al4V powder's temperature-dependent thermal conductivity k_p, as the heat transfer coefficient h_1, at the powder layer's outer surfaces.

$$h_1 = k_p (T) \qquad \cdots\cdots\cdots\cdots(4)$$

2.2 Mechanical model

- Stress Equilibrium

After completion of the simulation, the thermal model yields the temperature history for each nodal point; the quasi-static stress equilibrium is determined for each step. The governing stress equilibrium equation is given by (Gouge et al., 2018).

$$\nabla . \sigma = 0 \qquad \cdots\cdots\cdots\cdots(5)$$

where σ is the stress tensor and,

$$\sigma = \mathrm{D}\varepsilon_e \qquad \cdots\cdots\cdots(6)$$

where D is the material stiffness tensor, and ε_e is the elastic strain tensor.

- Mechanical properties of model

The material properties used to model the mechanical model are the temperature-dependent coefficient of linear thermal expansion α, Youngs modulus E, yield stress σ_y and poisons ratio v. The temperature-dependent mechanical properties of Ti6Al4V were taken from the work of (Rangaswamy et al., 2000). Poisson's ratio is assumed to be 0.342 in the elastic region and 0.49 in the plastic region. The plastic behaviour of the mechanical model was modelled using the assumption that the material is a linear isotropic strain-hardening material. The material properties used to define plasticity are the yield strength and the plastic tangent modulus.

3. Results and Discussion

3.1 Model validation

Firstly, the ABAQUS Thermal FE model was validated by comparing the melt pool dimensions of the FEA model with the experimental melt pool dimensions based on the work of Ali (2018), wherein the melt pool dimensions of a melted 50 μm layer of Ti6Al4V, built using optimised build parameters, was determined. The primary build parameters used were a laser power of 200 W, a scan speed of 640 mm/s and a laser spot size of 100 μm. Fig. 3. shows a comparison of the experimentally obtained and the Thermal FE
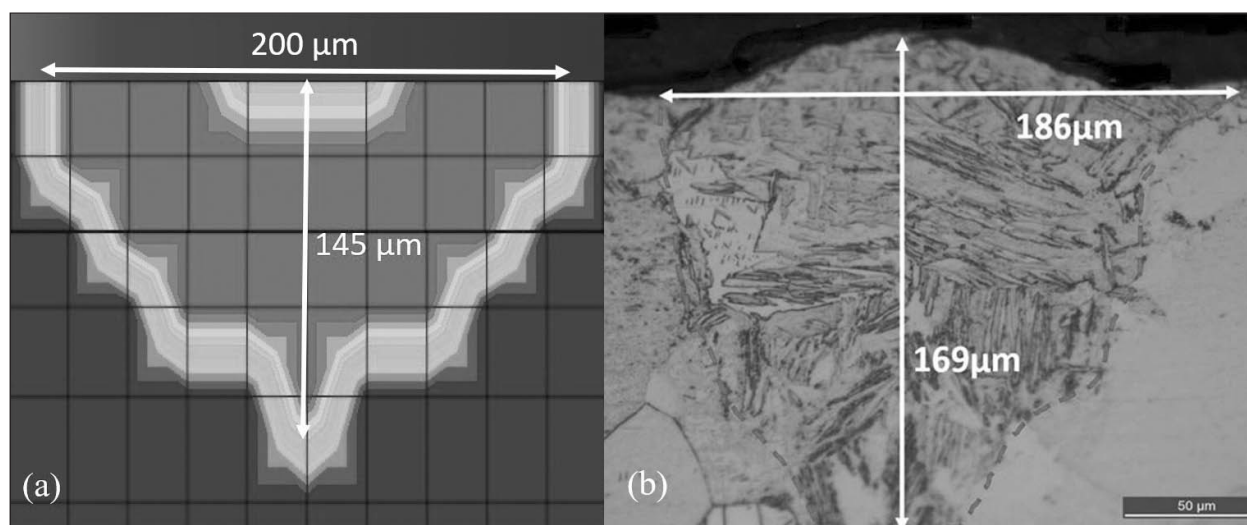

Fig. 3. a. Melt-pool dimensions predicted by the thermal FE model.
b. Experimentally measured melt-pool dimensions taken from Ali (2018).

model predicted melt pool dimensions for the exact build parameters, and we observe that they almost correlate with each other.

Secondly, the longitudinal stress pattern over the surface of a multi-layer FE Mechanical model was compared with the experimentally measured longitudinal stress values along a central straight line over the surface of an LPBF fabricated Ti6Al4V component of dimensions 60 × 20 × 8 mm built using Renishaw AM400 machine, using optimum processing parameters and a preheating temperature of 200℃. The residual stress measurement over the surface of the fabricated component was done using the XRD technique. The experimental longitudinal stress profile correlates with the one obtained using the FE model, with the maximum longitudinal stress concentration occurring in the middle part of the component, as seen in Fig. 4.

3.2 Effect of preheating on residual stresses

In some instances, the addition of preheating to the base platform during the LPBF process is observed as beneficial in reducing the residual stresses in the components. However, in most of the industrially available LPBF machines, the maximum preheating temperature is limited to around 400℃ due to various limitations. To better understand the effects of base platform preheating, we have used the FEA models to investigate the residual stresses over the top surface of a single-layer model built using the same process parameters but by varying the preheating temperature to up to 600℃.

Fig. 5. shows the Longitudinal Stress Profile across the surface of the single-layer model for a preheating temperature of 200℃ obtained using the FEA Thermo-Mechanical model. We have recorded the longitudinal stress values along four parallel paths over the model's surface, as shown in Fig. 5. The comparison of average values of Longitudinal residual stresses along the X direction for all three preheating cases is shown in Fig. 6.

Fig. 7. shows the Transverse residual stress profile across the surface of the single-layer model for a preheating temperature of 200℃ obtained using the FEA Thermo-Mechanical model. We have recorded the Transverse stress values along four parallel paths over the model's surface, as shown in Fig. 7. The comparison of average values of Transverse residual stresses along the Y direction for all three preheating cases is shown in Fig. 8.

We observe that as the preheat temperature of the build platform increases, the mean and maximum values of longitudinal and transverse residual stresses over the surface decrease, possibly due to a reduction in the thermal gradients across the component. The yield strength of solid Ti6Al4V, i.e., σ_y is considered to be 1100 MPa. As the preheat temperature increases from 200 to 400℃, we see a drop in mean longitudinal residual stress by up to 3%. However, as the preheat temperature is raised to 600℃, we see a much more significant drop in mean longitudinal stress by up to 18% and a sharp drop in the maximum longitudinal stress values by up to 20%. A similar trend is observed in the case of transverse residual stresses when the preheating temperature is increased, and at 600 ℃, the transverse residual stresses reduce and become compressive in nature. The magnitude of residual stresses over the surface of the experimentally fabricated part is lower when compared to the FEA model. This is because the stresses in the fabricated part have been measured once they have been cut off from the base platform using wire cut EDM process after the completion of the 3D printing process. The removal of the part from the base platform relieves the built-up residual stresses to some extent.
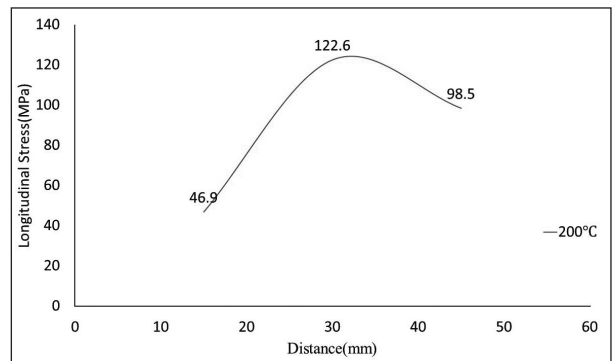

Fig. 4. Longitudinal stress profile over the top surface of LPBF fabricated component subjected to a preheating temperature of 200℃.

Table 1
FEA results for longitudinal surface residual stresses.

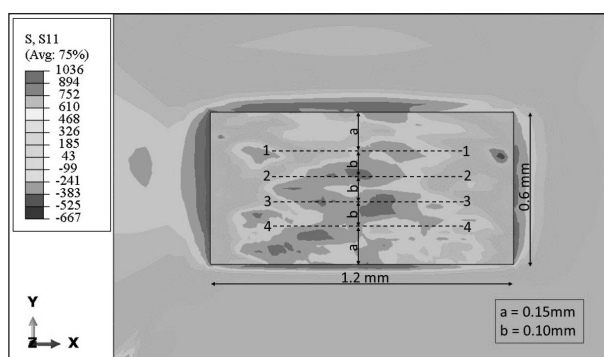| Temperature	Longitudinal Stress (MPa)	
	Average Stress	Maximum Stress
200℃	604(0.55σ_y)	709(0.64σ_y)
400℃	584(0.53σ_y)	663(0.60σ_y)
600℃	495(0.45σ_y)	562(0.51σ_y)

Fig. 5. Longitudinal stress profile over the top surface of a single layer FEA TM model subjected to a preheating temperature of 200℃.
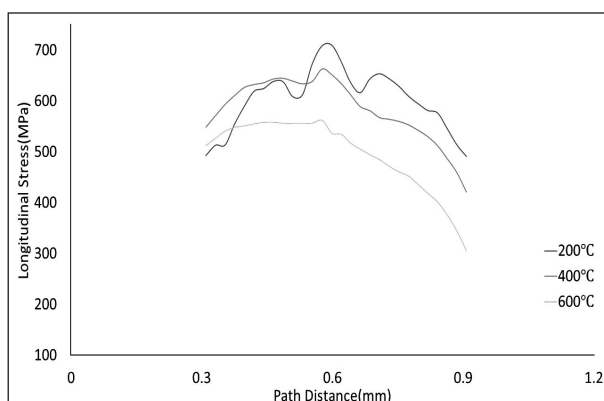

Fig. 6. Average longitudinal stress along the path for a single-layer model for varying preheat temperatures.
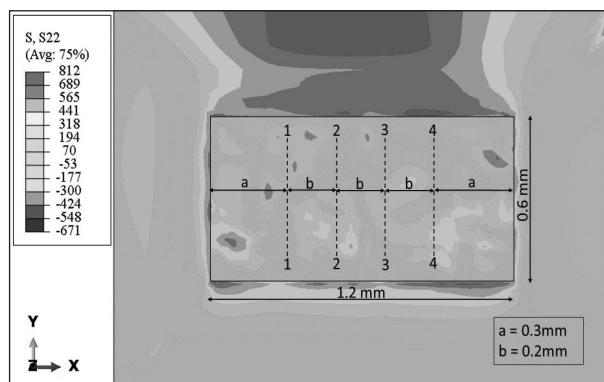

Fig. 7. Transverse stress profile over the top surface of a single layer FEA TM model subjected to a preheating temperature of 200℃.

Table 2
FEA results for transverse surface residual stresses.

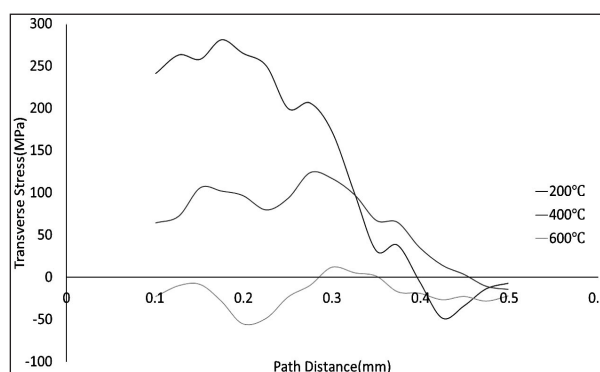| Temperature	Transverse Stress (MPa)	
	Average Stress	**Maximum Stress**
200℃	129(0.12σ_y)	281(0.25σ_y)
400℃	66(0.06σ_y)	124(0.11σ_y)
600℃	-18(0.02σ_y)	-22(0.02σ_y)

Fig. 8. Average transverse stress along the path for a single-layer model for varying preheat temperatures.

Acknowledgements

References

Alderson, N. A. (2012). Thermal Modeling and Simulation of Electron Beam Melting for Rapid Prototyping on Ti6Al4V Alloys, [Doctoral dissertation, North Carolina State University].

Ali, H., Ghadbeigi, H. & Mumtaz, K. (2018). Residual stress development in selective laser-melted Ti6Al4V: a parametric thermal modelling approach. *International Journal of Advanced Manufacturing Technology, 97,* 2621-2633.

Boivineau, M., Cagran, C., Doytier, D. et al. (2006). Thermophysical Properties of Solid and Liquid Ti-6Al-4V (TA6V) Alloy. *International Journal of Thermophysics, 27*(2), 507-529. https://doi.org/10.1007/PL00021868

Dunbar, A. J., Denlinger, E. R., Gouge, M.F., & Michaleris, P. (2016). Experimental validation of finite element modeling for laser powder bed fusion deformation. *Additive Manufacturing, 12,* 108-120.

Gouge, M. F., Michaleris, P., Denlinger, E. R., & Irwin, J. E. (2016). The Finite Element Method for the Thermo-Mechanical Modeling of Additive Manufacturing Processes. *Thermo-Mechanical Modeling of Additive Manufacturing,* (19-38). Elsevier BV.

Liu, S., Zhu, H., Peng, G., Yin, J., & Zeng, X. (2018). Microstructure Prediction of Selective Laser Melting AlSi10Mg Using Finite Element Analysis. *Materials & Design, 142*, 319-328.

Parry, L., Ashcroft, I. A., & Wildman, R. D. (2016). Understanding the effect of laser scan strategy

on residual stress in selective laser melting through thermo-mechanical simulation. *Additive Manufacturing, 12*(A), 1-15.

Rangaswamy, P., Choo, H., Prime, M.B., Bourke, M.A.M., & Larsen, J.M. (2000). High Temperature Stress Assessment in SCS-6/Ti-6A1-4V Composite Using Neutron Diffraction and Finite Element Modeling. *THERMEC International Conference.*

Safdar, S., Pinkerton, A.J., Li, L., Sheikh, M.A., & Withers, P.J. (2013). An anisotropic enhanced thermal conductivity approach for modelling laser melt pools for Ni-base super alloys. *Applied Mathematical Modelling, 37*(3), 1187-1195.

G. C. Akshay Kiran is an M. S. Research Scholar in the Department of Mechanical Engineering at IIT Madras. His current area of research is Thermo-Mechanical Modelling of the Laser Powder Bed Fusion AM Process. His other area of interest includes Aerodynamics, Additive manufacturing, Computer-Aided manufacturing, and FE analysis of mechanical systems.

Dr. Ramesh Babu N is a V. Balaraman Institute Chair Professor in the Department of Mechanical Engineering at IIT Madras. He obtained his Ph.D from IIT Madras in 1990. His research interest includes Manufacturing Technology, Grinding, Abrasive Waterjet Machining, Sheet metal fabrication, Laser Beam Machining, CNC, PLCs & Robotics, Precision Machine Tool development, Process modelling and simulation of manufacturing systems. (E-mail: nrbabu@smail.iitm.ac.in)